

Extended x-ray-absorption fine-structure study of $\text{La}_{2-x}\text{Sr}_x\text{CuO}_{4-y}$ superconductors

J. M. Tranquada, S. M. Heald, and A. R. Moodenbaugh

Brookhaven National Laboratory, Upton, New York 11973

(Received 28 August 1987)

From measurements of extended x-ray-absorption fine structure at the Cu K edge between 10 and 300 K, we have determined the temperature dependence of the mean-square relative displacements σ^2 for Cu—O, Cu—La, and Cu—Cu near neighbors in $\text{La}_{2-x}\text{Sr}_x\text{CuO}_{4-y}$ with $x=0, 0.15,$ and 0.3 . It is found that σ^2 for Cu—O and Cu—La neighbors shows little variation with x . Model calculations are used to demonstrate that $\sigma_{\text{Cu—O}}^2$ is sensitive to softening of the Cu—O breathing mode which has been predicted to be important for superconductivity in these materials. The Cu—O bonding is observed to be quite strong and no evidence is found for any significant change in the breathing-mode frequency with doping.

I. INTRODUCTION

The discoveries^{1,2} of high-temperature superconductivity in several copper oxides have come as a pleasant surprise to theorists who had previously predicted an upper limit of ~ 30 K for the transition temperature T_c assuming electron-phonon coupling, and have caused a great deal of speculation on possible new electron-pairing mechanisms. As the electron-phonon interaction is the only verified mechanism of superconductivity in all previously studied materials, it is logical to first see whether or not it may be able to explain the new phenomenon. Several band-structure calculations³⁻⁵ and analyses^{6,7} have been performed for the $\text{La}_{2-x}(\text{Ba},\text{Sr})_x\text{CuO}_{4-y}$ system, indicating how such coupling might occur.

The structure of $\text{La}_{2-x}(\text{Ba},\text{Sr})_x\text{CuO}_{4-y}$ consists of alternating layers of $\text{La}_{2-x}(\text{Ba},\text{Sr})_x\text{O}_2$ and CuO_2 planes.⁸⁻¹⁰ The structure is tetragonal for high temperatures and/or large x , while an orthorhombic distortion occurs at small x . The band-structure calculations³⁻⁵ indicate that the valence-band structure is dominated by hybridization between Cu $3d$ and O $2p$ states. The topmost band, which is the only one to cross the Fermi energy, is formed from Cu $3d_{x^2-y^2}$ and O $2p_{x,y}$ states within the CuO_2 planes. For the half-filled band case, corresponding to $x=y=0$, the Fermi surface is nested and a Peierls transition is predicted. As x increases the degree of Fermi-surface nesting is reduced, removing the requirement of a structural transition, but still resulting in a strong electron-phonon coupling which would be responsible for the superconductivity.

Early on it was believed that the orthorhombic distortion might be the predicted Peierls phase.^{4,8} Assuming the tetragonal-to-orthorhombic transition to be electronically driven, the phases should be related by a soft-phonon mode. Weber⁶ has shown that the mode having the strongest coupling to the electrons involves a "breathing"-mode displacement of the oxygen atoms with respect to the copper within the CuO_2 planes. Stavola, Cava, and Rietman¹¹ interpreted their Raman measurements in $\text{La}_{2-x}\text{Sr}_x\text{CuO}_{4-y}$ as evidence of such a frozen-in breathing-mode distortion for small x . However, the feature assigned to the extra mode was also present in the

high-temperature tetragonal phase of La_2CuO_4 , in which such a distortion is inconsistent with the crystal symmetry. (An alternative explanation for the x dependence of the peak in question was given in an added note.)

In a recent neutron scattering study on single crystals with x near zero, Birgeneau *et al.*¹² have demonstrated that the transition does occur via a soft-mode mechanism but that no breathing-mode distortion is present. Observations of softening in Young's modulus¹³ and sound velocity¹⁴ measurements in $x=0.15$ compounds near the orthorhombic-to-tetragonal transition temperature presumably reflect the same effect.

The negative result obtained in searches^{15,16} for an isotope effect in $\text{YBa}_2\text{Cu}_3\text{O}_7$ has cast some doubt on the importance of phonons for superconductivity in that material. However, a significant reduction in T_c due to partial replacement of ^{16}O by ^{18}O in $\text{La}_{1.85}\text{Sr}_{0.15}\text{CuO}_4$ has now been observed and interpreted in terms of a strong electron-phonon interaction.^{17,18} Furthermore, the observation¹⁹ of anomalous variations in the orthorhombic distortion near T_c , as well as the fact that the orthorhombic-to-tetragonal transition temperature approaches T_c as x increases to the point of maximum T_c ($x \approx 0.15$), continues to keep the electron-phonon issue alive.

To better resolve things, it is important to check experimentally to see whether any anomalies exist in the phonon modes which are expected to be relevant. Measurements of the phonon densities of states in $\text{La}_{1.85}\text{Sr}_{0.15}\text{CuO}_4$ and La_2CuO_4 have been made by Renker *et al.*²⁰ using inelastic neutron scattering from powders. They found evidence for a slight softening of some optical modes, but the specific modes affected were not directly identifiable. The Cu—O breathing mode predicted to be important is at the zone boundary and hence cannot be directly probed by ir or Raman spectroscopies.

In this paper we present an extended x-ray-absorption fine-structure (EXAFS) study of lattice dynamics in $\text{La}_{2-x}\text{Sr}_x\text{CuO}_{4-y}$ for $x=0, 0.15,$ and 0.3 at temperatures between 10 K and room temperature. The mean-square relative displacements σ^2 for Cu—O and Cu—Cu near neighbors provide good measures of bonding within the CuO_2 plane, and $\sigma_{\text{Cu—O}}^2$ contains a significant contribution from the breathing mode. We find no evidence for soften-

ing of the Cu—O bond in the $x=0.15$ material relative to the $x=0$ or 0.3 samples. A brief description of this work has previously appeared.²¹

The sample preparation and characterization as well as the experimental procedure have been discussed previously.²² We begin with a review of the theory of the EXAFS temperature dependence and the information which it contains. The analysis of the data is then discussed and experimental results are presented. Next, calculations using a simple lattice-dynamical model are described and compared with the data. Finally, the results and their significance are discussed and summarized.

II. THEORY OF EXAFS TEMPERATURE DEPENDENCE

The general theory and interpretation of EXAFS are now well established^{23,24} and will not be discussed in detail. Here we wish to concentrate on the temperature dependence of the fine structure. As the EXAFS interference function $\chi(k)$ consists of a sum of scattering contributions from coordination shells of atoms surrounding the x-ray-absorption site, displacements of atoms within a shell relative to a mean coordination distance will cause a smearing of the interference function and a reduction in the net scattering amplitude. Motions of the atoms due to thermal (as well as zero-point) vibrations always cause some amplitude reduction, and static displacements can also be important. As long as the relative displacements are sufficiently small, their effect on the fine-structure amplitude is well described by a Debye-Waller-like factor, $\exp(-2k^2\sigma_n^2)$, where σ_n^2 is the mean-square relative displacement for the n th shell and the photoelectron wave vector k is related to the photoelectron's energy E by $k=(2m_e E/\hbar^2)^{1/2}$.

The mean-square relative displacement is defined by

$$\sigma_n^2 = \langle [(\mathbf{u}_n - \mathbf{u}_0) \cdot \hat{\mathbf{R}}_n]^2 \rangle, \quad (1)$$

where \mathbf{u}_n and \mathbf{u}_0 are displacement vectors relative to the mean atomic positions for a particular atom in the n th shell and the absorbing atom, respectively, \mathbf{R}_n is a vector connecting the two sites, $\hat{\mathbf{R}}_n$ is a unit vector in the same direction, and the angle brackets denote a thermal average. If static displacements occur, one must also perform a configuration average. By transforming to normal coordinates, one can convert Eq. (1) into a thermal average over a projected density of phonon modes $\rho_n(\omega)$:²⁵

$$\sigma_n^2(T) = \frac{\hbar}{2\mu_n} \int d\omega \frac{\rho_n(\omega)}{\omega} \coth \left(\frac{\hbar\omega}{2k_B T} \right), \quad (2)$$

where

$$\rho_n(\omega) = \frac{1}{N} \sum_{q,j} P_n(\mathbf{q}j) \delta(\omega - \omega_j(\mathbf{q})), \quad (3)$$

$\omega_j(\mathbf{q})$ is the frequency of a phonon with wave vector \mathbf{q} and mode j , the reduced mass μ_n is related to the atomic masses m_n and m_0 by $\mu_n^{-1} = m_n^{-1} + m_0^{-1}$, and N is the number of atoms in the crystal. The general formula for

the projection factor is²⁶

$$P_n(\mathbf{q}j) = \left| \left[\left(\frac{\mu_n}{m_n} \right)^{1/2} e^{i\mathbf{q} \cdot \mathbf{R}_n} \hat{\mathbf{e}}_n(\mathbf{q}j) \cdot \hat{\mathbf{R}}_n - \left(\frac{\mu_n}{m_0} \right)^{1/2} \hat{\mathbf{e}}_0(\mathbf{q}j) \cdot \hat{\mathbf{R}}_n \right]^2 \right|, \quad (4)$$

where $\hat{\mathbf{e}}_n(\mathbf{q}j)$ and $\hat{\mathbf{e}}_0(\mathbf{q}j)$ are normalized phonon eigenvectors. When performing numerical calculations using these formulas it is useful to know that the projected densities of states satisfy the sum rule

$$\int_0^\infty d\omega \rho_n(\omega) = 1. \quad (5)$$

Equations (2)–(4) show that σ_n^2 contains information about lattice vibrations in a crystal. While the phonon density of states and dispersion relations can be determined more directly with techniques such as inelastic neutron scattering, Eq. (4) shows that σ_n^2 also contains information about phonon eigenvectors, which is not directly obtainable with most other techniques. EXAFS measurements also do not require large samples or single crystals. The complementarity of EXAFS and neutron scattering techniques has recently been demonstrated in lattice-dynamical studies of UBe_{13} .^{27,28}

If a force-constant model exists, one can calculate the mean-square relative displacements directly and compare with experiment. Often times such calculations are not practical, and it may be more convenient to parametrize the measurements in terms of a simple model. A particularly useful one, especially for near neighbors, is the Einstein model,²⁵ in which one approximates the projected density of states as

$$\rho_n(\omega) = \delta(\omega - \omega_n^E), \quad (6)$$

where $\delta(\omega)$ is a Dirac delta function. Substituting into Eq. (2), one obtains the simple formula

$$\sigma_n^2(T) = \frac{\hbar}{2\mu_n \omega_n^E} \coth(\hbar\omega_n^E/2k_B T). \quad (7)$$

Note that this model is different from the original Einstein approximation for describing the specific heat at low temperatures in which all atoms are assumed to vibrate independently but with the same frequency; here, it is assumed that all of the relevant atom *pairs* vibrate independently at the same frequency. Actually, the approximation has somewhat more general validity, and in certain opportune cases involving nearest-neighbor pairs it is possible to relate ω_E directly to a nearest-neighbor force constant.^{29,30}

On the practical side, it should be pointed out that at the present time absolute determinations of σ_n^2 generally have very large uncertainties, limiting the usefulness of such results. However, the temperature dependence of σ_n^2 in a single compound or in a group of closely related materials can be determined with relatively good precision. As a result, our analysis will focus on the temperature dependent part of σ_n^2 .

III. DATA ANALYSIS

Working at beam line X-11 of the National Synchrotron Light Source (NSLS), EXAFS measurements were made at the Cu K edge in $\text{La}_{2-x}\text{Sr}_x\text{CuO}_{4-y}$ for $x=0, 0.15, \text{ and } 0.3$ at temperatures between 10 K and room temperature. The interference function $\chi(k)$ was extracted from each data set using standard techniques.^{23,24} The similarity between the Fourier-transformed data measured at 10 K on the undoped and $x=0.15$ samples has previously been illustrated.²¹ Figure 1(a) shows the magnitude of Fourier transforms of $k^2\chi(k)$ (k range of 2.0–17.7 \AA^{-1}) for $x=0.15$ at roughly 100-K intervals over the measured temperature range. The approximate radial distribution of atoms about Cu, determined from a diffraction study,⁸ is listed in Table I. The coordination shell peaks in Fig. 1 are shifted to lower R from their correct crystallographic distances due to scattering phase shifts. Figure 1(b) shows the same data transformed as $k^3\chi(k)$ multiplied by a Gaussian centered on the k -range window and decaying to 0.1 at the window edges. The higher k weighting emphasizes the metal atom shells, while the Gaussian window reduces the ripple and long tails around the peaks due to transforming over a finite k range. In both (a) and (b) the first O, La(Sr), and Cu shells are quite prominent, with the oxygen peak, which is due predominantly to the four O neighbors within a CuO_2 plane, showing very little temperature dependence. The in-plane Cu shell shows a somewhat larger effect, while the out-of-plane La shows the largest damping with temperature. This pattern is repeated in higher shells, with no significant scattering contribution observed from out-of-plane Cu shells. Note that Cu atoms along [100] and

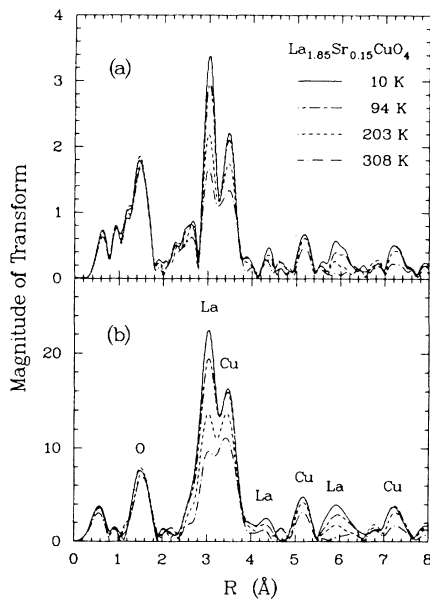


FIG. 1. Magnitudes of Fourier transforms of $\chi(k)$ measured at the Cu K edge for $\text{La}_{1.85}\text{Sr}_{0.15}\text{CuO}_4$ at approximately 100-K intervals. (a) Transforms of $k^2\chi(k)$. (b) Transforms of $k^3\chi(k)$ multiplied by a Gaussian k window as discussed in the text. Some of the coordination shells are labeled in (b).

TABLE I. Radial distribution of atoms about the copper site in $\text{La}_{2-x}\text{Sr}_x\text{CuO}_{4-y}$. Only selected shells beyond the first four are listed and their shell indices are arbitrary. Typical position vector coordinates are listed in the fourth column in units of (a, a, c) where a and c are the tetragonal lattice parameters.

Shell	Atom	Coordination number	(l, m, n)	Distance (\AA)
1	O	4	$(\frac{1}{2}, 0, 0)$	1.9
2	O	2	$(0, 0, u_0)$	2.4
3	La (Sr)	8	$(\frac{1}{2}, \frac{1}{2}, u_{\text{La}})$	3.2
4	Cu	4	$(1, 0, 0)$	3.8
5	La (Sr)	2	$(0, 0, \frac{1}{2} - u_{\text{La}})$	4.8
6	Cu	4	$(1, 1, 0)$	5.3
7	La (Sr)	8	$(1, 0, \frac{1}{2} - u_{\text{La}})$	6.1
	La (Sr)	16	$(\frac{3}{2}, \frac{1}{2}, u_{\text{La}})$	6.3
8	Cu	4	$(2, 0, 0)$	7.6

[010] directions are shadowed by intervening O atoms which enhance the effective scattering due to the “focusing” effect.

To quantify the temperature-dependent changes, the first three peaks were individually Fourier transformed back to k space and analyzed using the “ratio” method.³¹ The O peak was filtered using k^2 weighting and a rectangular R -space window covering 0.8–2.0 \AA . The La(Sr) and Cu peaks were filtered with k^3 weighting, no Gaussian k window, and R -space windows of 2.3–3.3 \AA and 3.3–3.8 \AA , respectively. Although the Cu and La shells are not well separated, we believe that the temperature dependence of the interatomic distances and σ_n^2 can be obtained with reasonable accuracy.

As mentioned above, the Cu–O peak in Fig. 1 is due predominantly to the four in-plane O neighbors. We have compared the amplitude of the filtered shell at 10 K for each sample with the Cu–O shell extracted from a 10-K measurement on Cu_2O . Assuming that in Cu_2O the amplitude corresponds to the known coordination number of two and correcting for the R^{-2} factor, the coordination found in the $\text{La}_{2-x}\text{Sr}_x\text{CuO}_{4-y}$ samples is 4.2 ± 0.2 , indicating that the EXAFS is relatively insensitive to the two oxygens along the c axis. Figure 2 shows the Cu–O single shell amplitude for $x=0.15$. Interference from the two oxygens should cause “beating,”³² with minima occurring at $k \sim 3$ and 9.5 \AA^{-1} . The lack of any significant dips at these positions is further evidence that only the in-plane oxygens are observed. In R space, it is likely that the contribution from the c -axis oxygens at least partially overlaps the peak at $\sim 2.5 \text{ \AA}$ which is a side lobe of the La peak due to minima in the La backscattering amplitude, as shown in Fig. 2. The overlapping part cannot be isolated and is excluded from the filtered shell. Furthermore, neutron scattering measurements^{33,34} indicate that the thermal parameter for these atoms is quite a bit larger than for the in-plane oxygens. Finally, the Cu–O shell from Cu_2O did not appear sufficiently transferrable to justify two-shell fitting as was performed by Boyce *et al.*³⁵ We have assumed that the temperature dependence of the

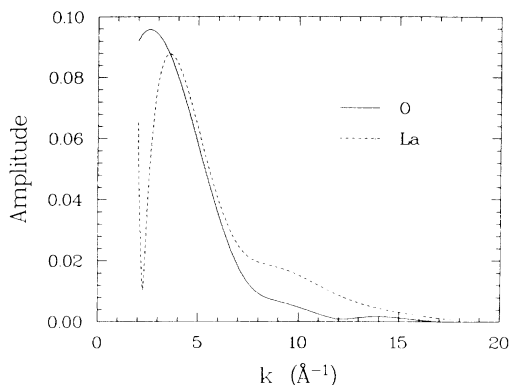


FIG. 2. Fourier-filtered single-shell amplitudes for near-neighbor O and La shells in La_2CuO_4 .

filtered Cu—O shell is due entirely to in-plane atoms.

In the ratio method, for a given shell the change in σ^2 between two measurements is obtained from the ratio of the single-shell amplitudes. When plotted versus k^2 the ratio should be a straight line with a slope of $2\Delta\sigma^2$. In the present case, the ratio should intercept the origin at $k=0$; any deviations should be due to measurement or normalization errors. In practice, noise and artifacts of the Fourier filtering process can cause straight-line fits to the ratios to have a slightly nonzero y intercept. In order to obtain consistent results, all linear fits were forced to have a y intercept of zero. The fits were performed over a k range of 3.5 – 16 \AA^{-1} and were weighted by error bars determined from multiple (2–3) measurements of each sample at a given temperature.

For the O and Cu shells, all ratio fits were performed relative to the 10-K measurement on La_2CuO_4 . This approach was not appropriate for the La(Sr) shell, since the variable doping caused a change in the effective La(Sr) backscattering amplitude between samples. Instead, the La(Sr) ratios were referenced to the 10-K data for each sample. The results are plotted in Fig. 3. For each shell, the temperature dependence of σ^2 varies very little among the three samples. The differences between shells agree with the trends observed in Fig. 1. The lowest values in each case occur for $x=0.15$. The slightly larger values of $\sigma_{\text{Cu-O}}^2$ and $\sigma_{\text{Cu-Cu}}^2$ for the $x=0.3$ sample could be due to a small amount of static disorder due to the greater level of doping. The greater temperature dependence of $\sigma_{\text{Cu-Cu}}^2$ for the undoped sample is probably due to the dimpling of the CuO_2 planes in the orthorhombic structure. The results for the Cu—O shell are quite similar to those obtained by Boyce *et al.*³⁵ for $x=0.15$.

The solid lines in Fig. 3 represent Einstein model fits to the $x=0.15$ data. The Einstein frequencies obtained are $603 \pm 27 \text{ K}$, $242 \pm 4 \text{ K}$, and $349 \pm 14 \text{ K}$ for Cu—O, Cu—La, and Cu—Cu, respectively. The bonding within the CuO_2 planes is clearly quite strong, with weaker bonding between planes.

We have also determined the temperature dependences of the interatomic distances by taking differences between single-shell phases. The results are shown in Fig. 4. The

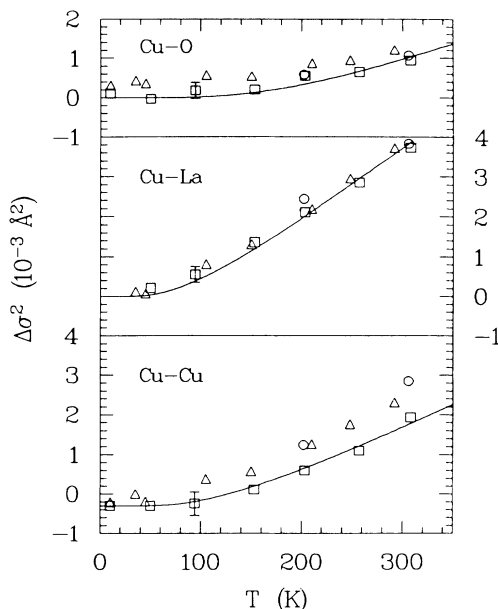


FIG. 3. Temperature dependence of σ^2 for Cu—O, Cu—La, and Cu—Cu shells in $\text{La}_{2-x}\text{Sr}_x\text{CuO}_{4-y}$: circles, $x=0$; squares, $x=0.15$; triangles, $x=0.3$.

dashed lines indicate the thermal expansion measured macroscopically on an $x=0.15$ sample by Fleming, Batlogg, Cava, and Rietman.¹⁰ For each shell and sample, the temperature dependence is consistent with the thermal expansion data and the results of Boyce *et al.*³⁵ for an $x=0.15$ sample. A much larger change is observed in Cu—O and Cu—Cu distances in going from $x=0$ to

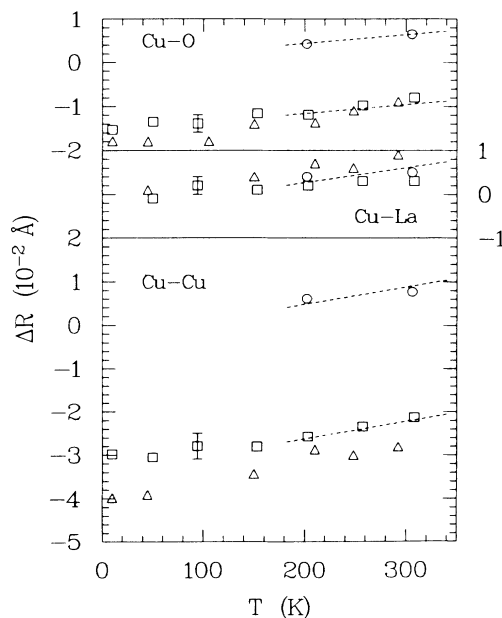


FIG. 4. Temperature dependence of interatomic distance R for Cu—O, Cu—La, and Cu—Cu shells in $\text{La}_{2-x}\text{Sr}_x\text{CuO}_{4-y}$. Circles: $x=0$; squares: $x=0.15$; triangles: $x=0.3$.

$x=0.15$ than in going from 0.15 to 0.3. This result is consistent with the x-ray diffraction study of Kanbe *et al.*³⁶ who found that the a lattice parameter stopped decreasing with x and remained constant for $x \gtrsim 0.2$. They suggested that this break might occur due to reaching a solubility limit.

It is interesting to note that from the analysis of neutron-diffraction measurements on an $x=0.15$ sample, Cava, Santoro, Johnson, and Rhodes³⁷ find that the in-plane Cu–O distance changes by only 0.0003 ± 0.0001 Å between 10 and 300 K. The change which we observe is twenty times larger. We cannot help but question the extreme precision with which the neutron results are quoted.

IV. MODEL CALCULATIONS

It was shown in the last section that there is very little variation in the temperature dependence of $\sigma_{\text{Cu-O}}^2$ as a function of doping level x . We wish to relate this observation to possible changes in particular phonon modes; however, σ^2 involves an average over the Brillouin zone [cf. Eqs. (2)–(4)], and the soft breathing modes predicted by Weber occur in only a small part of that volume. To determine the sensitivity of EXAFS measurements to soft breathing modes, we have performed calculations using a simple two-dimensional force-constant model for the CuO_2 planes. The model consists of a nearest-neighbor force between Cu and O atoms of strength $k_{\text{Cu-O}}$ and a next-nearest-neighbor (NNN) force between copper atoms of strength $k_{\text{Cu-Cu}}$. The in-plane motion of a Cu atom is likely to be partially constrained by bonds to its c -axis O neighbors, and the NNN force constant helps to mimic these neglected constraints. The in-plane O atoms are only allowed to move along the bond directions, so that there are just four degrees of freedom per unit cell.

To simulate the breathing-mode electron-phonon coupling, a breathing shell about each Cu atom was introduced.³⁸ The only degree of freedom for the shell is a radial dilation or contraction about the Cu core. A spring of strength of $k_{\text{Cu-O}}$ couples each oxygen to the Cu shell, as well as to the core, and a spring of strength k_{br} connects the Cu core and shell. When $k_{\text{br}} \rightarrow \infty$, one returns to the two-force-constant model, while small k_{br} corresponds to breathing-mode softening. In the usual breathing-shell model,³⁸ the force constant k_{br} appears in the dynamical matrix multiplied by a phase factor $\sin(q_x a/2)\sin(q_y a/2)$, where $\mathbf{q}=(q_x, q_y)$ is the phonon's wave vector. Using this standard \mathbf{q} dependence, it was found that soft breathing modes resulted in extremely large increases in $\sigma_{\text{Cu-O}}^2$, due largely to softening of low-frequency, small- q acoustic modes. Because our model is two-dimensional, with the density of states remaining finite at $\omega=0$, it was felt that the smaller- q modes might be contributing excessively relative to a proper three-dimensional calculation, and so the phase factor for the k_{br} term was arbitrarily changed from \sin^2 to \sin^4 .

We began the analysis by considering the case of $k_{\text{br}}=\infty$. Adjusting the two force constants by trial and error to obtain $\Delta\sigma^2$ values matching those observed for the $x=0.15$ sample, we arrived at the results shown in Fig. 5, with $k_{\text{Cu-O}}=7.5$ eV/Å² and $k_{\text{Cu-Cu}}=3.5$ eV/Å². The

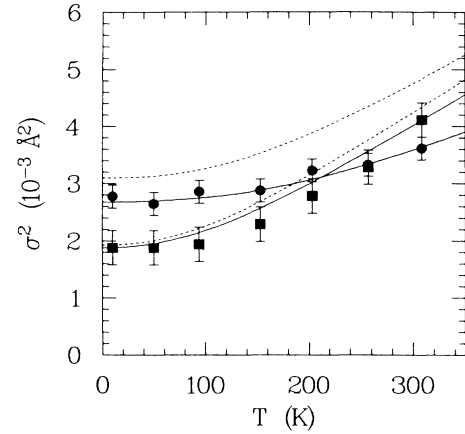


FIG. 5. Mean-square relative displacements measured for Cu–O (circles) and Cu–Cu (squares) near neighbors in $\text{La}_{1.85}\text{Sr}_{0.15}\text{CuO}_4$. The lines represent theoretical results as described in the text. The experimentally measured values of $\Delta\sigma^2$ have been shifted vertically to match the calculation.

solid curves correspond to the calculation and each set of data has been shifted vertically by a constant. The phonon dispersion along the $\mathbf{q}=(2\pi/a)(\xi, \xi, 0)$ direction is shown in Fig. 6. The two solid curves, which are each doubly degenerate, correspond to the present case.

Weber finds that for $x=0.15$ and $k_{\text{Cu-O}}=7.8$ eV/Å², the breathing mode at the X point of the Brillouin zone is reduced by about a factor of four. Simulating this softening with $k_{\text{br}}=1.6$ eV/Å², we find that the phonon branches are no longer degenerate along $(\xi, \xi, 0)$, and while two of the branches remain unchanged (solid curves), the other two (dashed curves) exhibit strong softening, as shown in Fig. 6. The projected densities of states for Cu–O nearest neighbors with (dashed curve) and without (solid curve) breathing-mode softening are plotted in Fig. 7. The high-frequency peak due to zone-center modes remains unchanged, while weight due to zone-boundary breathing

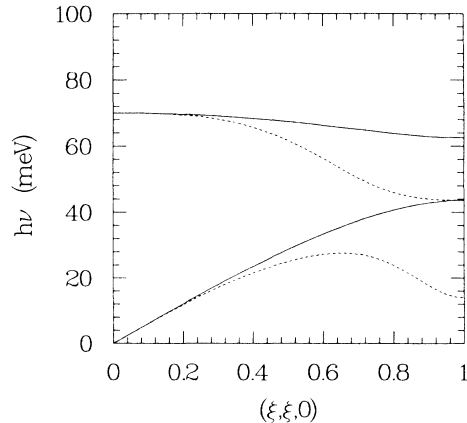


FIG. 6. Calculated phonon dispersion curves along $\mathbf{q}=(2\pi/a)(\xi, \xi, 0)$ in $\text{La}_{1.85}\text{Sr}_{0.15}\text{CuO}_4$ for the two-dimensional force-constant model discussed in the text.

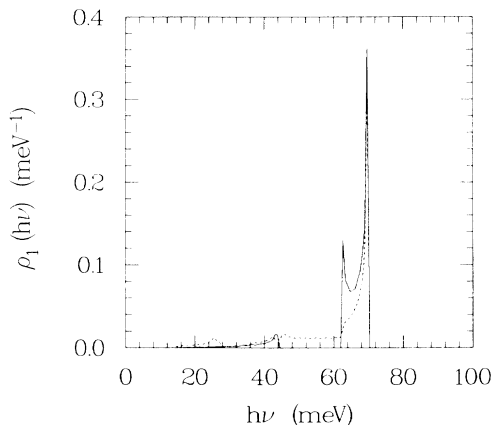


FIG. 7. Projected density of states for Cu–O nearest neighbors with $k_{\text{Cu-O}}=7.5 \text{ eV/\AA}^2$ and $k_{\text{Cu-Cu}}=3.5 \text{ eV/\AA}^2$. Solid line: $k_{\text{br}}=\infty$; dashed line: $k_{\text{br}}=1.6 \text{ eV/\AA}^2$.

modes shifts to much lower frequencies. The values of σ^2 for Cu–O and Cu–Cu pairs obtained in the softened case are indicated by the dashed lines in Fig. 5. While there is little change for Cu–Cu, the increase in the temperature dependence for Cu–O is quite large and should be easily detectable if present.

Although we conclude that extreme softening of the breathing mode does not occur, we cannot rule out a small but finite amount of electron-phonon coupling. Good agreement with the data can be obtained by adjusting $k_{\text{Cu-O}}$ and $k_{\text{Cu-Cu}}$ for a given value of k_{br} as long as k_{br} is not too small; decreasing k_{br} (increasing softening) requires that $k_{\text{Cu-O}}$ increase and $k_{\text{Cu-Cu}}$ decrease. However, if $k_{\text{Cu-O}}$ and $k_{\text{Cu-Cu}}$ are fixed, softening becomes detectable in $\sigma_{\text{Cu-O}}^2$ when the breathing-mode frequency is reduced by $\sim \frac{1}{3}$. The important point is, making the reasonable assumption that the actual $k_{\text{Cu-O}}$ does not vary, that there is no dramatic change in electron-phonon coupling with doping.

V. SUMMARY AND DISCUSSION

We have measured the temperature dependence of σ^2 for Cu–O, Cu–La, and Cu–Cu near neighbors in $\text{La}_{2-x}\text{Sr}_x\text{CuO}_{4-y}$ and have shown that there is little variation in these quantities as a function of x . The Cu–O bond is strong, with a characteristic frequency of approximately 600 K. Model calculations indicate that $\sigma_{\text{Cu-O}}^2$ is sensitive to breathing-mode contributions, and we conclude that any electron-phonon coupling is not extreme and does not vary with doping.

Weber's calculations⁶ of electron-phonon coupling, based on the band-structure results of Mattheiss,³ show that the dominant electron-phonon interaction involves

breathing-mode displacements of in-plane O atoms about the Cu. Furthermore, the electron-phonon coupling, and concomitant breathing-mode softening, is calculated to increase rapidly as x decreases, with the lattice becoming unstable to a breathing-mode Peierls distortion for $x \lesssim 0.1$. Our results clearly contradict this prediction. That a model for $\text{La}_{2-x}\text{Sr}_x\text{CuO}_{4-y}$ based on band-structure calculations which rely on the local density approximation does not agree with experiment comes as no surprise, as we have previously shown^{21,22} from x-ray-absorption near-edge measurements that the band-structure results do not give an accurate description of the electronic structure.

It should be noted that Fu and Freeman⁷ have performed a frozen-phonon calculation for the breathing-mode and find both a large electron-phonon coupling and a high phonon frequency, $\omega_{\text{br}} \approx 110 \text{ meV}$ (1250 K) for $x=0$. Such a frequency is certainly much larger than any found in our experiment or in the neutron study of Renker *et al.*²⁰ However, the calculations do indicate that for small x and small displacements the potential well is highly anharmonic, and perhaps some of the discrepancy with Weber's study involves the interpretation of the potential. Regardless of that, an anharmonic potential well should result in a strong temperature dependence of the phonon frequencies, which is not observed.

We conclude that the breathing-mode electron-phonon coupling is not strong enough to explain the high-temperature superconductivity in $\text{La}_{2-x}\text{Sr}_x\text{CuO}_{4-y}$. While a different phonon mode could possibly be important, an unanticipated way of coupling to the electrons would have to be found. Is it possible to reconcile this result with the observation of an isotope effect in the $x=0.15$ compound? In the usual interpretation of the isotope effect,³⁹ it is assumed that purely electronic interactions are repulsive and the attractive interaction is due solely to phonon exchange. Alternatively, Emery⁴⁰ has pointed out that if attractive interactions are due predominantly to electron-electron effects, with phonons making only a minor contribution, a significant isotope effect is still possible and even likely. The surprise in this case is that no isotope effect is observed in the 90-K superconductors. Certainly with the large Cu–O relative motion ($\gtrsim 0.05 \text{ \AA}$, due largely to the small oxygen mass) one would expect phonons to have some effect on the electron pairing; however, we believe it is likely that an explanation of high- T_c superconductivity will require a nonphonon mechanism.

ACKNOWLEDGMENTS

Discussions with W. Weber and V. J. Emery are gratefully acknowledged. This work was performed on beam line X-11 at the NSLS, Brookhaven Laboratory, and is supported by the U.S. Department of Energy under Contracts No. DE-AC02-76CH00016 and No. DE-AS05-80-ER10742.

- ¹J. G. Bednorz and K. A. Müller, *Z. Phys. B* **64**, 189 (1986).
- ²M. K. Wu, J. R. Ashburn, C. J. Torng, P. H. Hor, R. L. Meng, L. Gao, Z. J. Huang, Y. Q. Wang, and C. W. Chu, *Phys. Rev. Lett.* **58**, 908 (1987).
- ³L. F. Mattheiss, *Phys. Rev. Lett.* **58**, 1028 (1987).
- ⁴J. Yu, A. J. Freeman, and J.-H. Xu, *Phys. Rev. Lett.* **58**, 1035 (1987).
- ⁵W. E. Pickett, H. Krakauer, D. A. Papaconstantopoulos, and L. L. Boyer, *Phys. Rev. B* **35**, 7252 (1987).
- ⁶W. Weber, *Phys. Rev. Lett.* **58**, 1371 (1987).
- ⁷C. L. Fu and A. J. Freeman, *Phys. Rev. B* **35**, 8861 (1987).
- ⁸J. D. Jorgensen, H.-B. Schüttler, D. G. Hinks, D. W. Capone II, K. Zhang, and M. B. Brodsky, *Phys. Rev. Lett.* **58**, 1024 (1987).
- ⁹V. B. Grande, Hk. Müller-Buschbaum, and M. Schweizer, *Z. Anorg. Allg. Chem.* **428**, 120 (1977).
- ¹⁰R. M. Fleming, B. Batlogg, R. J. Cava, and E. A. Rietman, *Phys. Rev. B* **35**, 7191 (1987).
- ¹¹M. Stavola, R. J. Cava, and E. A. Rietman, *Phys. Rev. Lett.* **58**, 1571 (1987).
- ¹²R. J. Birgeneau, C. Y. Chen, D. R. Gabbe, H. P. Jenssen, M. A. Kastner, C. J. Peters, P. J. Picone, T. Thio, T. R. Thurston, H. L. Tuller, J. D. Axe, P. Böni, and G. Shirane, *Phys. Rev. Lett.* **59**, 1329 (1987).
- ¹³L. C. Bourne, A. Zettl, K. J. Chang, M. L. Cohen, A. M. Stacy, and H. K. Ham, *Phys. Rev. B* **35**, 8785 (1987).
- ¹⁴D. J. Bishop, P. L. Gammel, A. P. Ramirez, R. J. Cava, B. Batlogg, and E. A. Rietman, *Phys. Rev. B* **35**, 8788 (1987).
- ¹⁵B. Batlogg, R. J. Cava, A. Jayaraman, R. B. van Dover, G. A. Kourouklis, S. Sunshine, D. W. Murphy, L. W. Rupp, H. S. Chen, A. White, K. T. Short, A. M. Muzsca, and E. A. Rietman, *Phys. Rev. Lett.* **58**, 2333 (1987).
- ¹⁶L. C. Bourne, M. F. Crommie, A. Zettl, H.-C. zur Loye, S. W. Keller, K. L. Leary, A. M. Stacy, K. J. Chang, M. L. Cohen, and D. E. Morris, *Phys. Rev. Lett.* **58**, 2337 (1987).
- ¹⁷B. Batlogg, G. Kourouklis, W. Weber, R. J. Cava, A. Jayaraman, A. E. White, K. T. Short, L. W. Rupp, and E. A. Rietman, *Phys. Rev. Lett.* **59**, 912 (1987).
- ¹⁸T. A. Faltens, W. K. Ham, S. W. Keller, K. J. Leary, J. N. Michaels, A. M. Stacy, H.-C. zur Loye, D. E. Morris, T. W. Barbee III, L. C. Bourne, M. L. Cohen, S. Hoen, and A. Zettl, *Phys. Rev. Lett.* **59**, 915 (1987).
- ¹⁹D. McK. Paul, G. Balakrishnan, N. R. Bernhoeft, W. I. F. David, and W. T. A. Harrison, *Phys. Rev. Lett.* **58**, 1976 (1987).
- ²⁰B. Renker, F. Gompf, E. Gering, N. Nücker, D. Ewert, W. Reichardt, and H. Rietschel, *Z. Phys. B* **67**, 15 (1987).
- ²¹J. M. Tranquada, S. M. Heald, A. R. Moodenbaugh, and M. Suenaga, *Phys. Rev. B* **35**, 7187 (1987).
- ²²J. M. Tranquada, S. M. Heald, and A. R. Moodenbaugh, *Phys. Rev. B* **36**, 5263 (1987).
- ²³E. A. Stern and S. M. Heald, in *Handbook on Synchrotron Radiation*, edited by E. E. Koch (North-Holland, Amsterdam, 1983), Vol. 1, p. 955.
- ²⁴P. A. Lee, P. H. Citrin, P. Eisenberger, and B. M. Kincaid, *Rev. Mod. Phys.* **53**, 769 (1981).
- ²⁵E. Sevillano, H. Meuth, and J. J. Rehr, *Phys. Rev. B* **20**, 4908 (1979).
- ²⁶J. M. Tranquada, Ph.D. thesis, University of Washington, 1983 (unpublished).
- ²⁷J. M. Tranquada, S. M. Heald, M. A. Pick, Z. Fisk, and J. L. Smith, *J. Phys. (Paris) Colloq.* **47**, C8-937 (1987).
- ²⁸B. Renker, F. Gompf, W. Reichardt, H. Rietschel, J. B. Suck, and J. Beuers, *Phys. Rev. B* **32**, 1859 (1985).
- ²⁹G. S. Knapp, H. K. Pan, and J. M. Tranquada, *Phys. Rev. B* **32**, 2006 (1985).
- ³⁰J. M. Tranquada and C. Y. Yang, *Solid State Commun.* **63**, 211 (1987).
- ³¹E. A. Stern, D. E. Sayers, and F. W. Lytle, *Phys. Rev. B* **11**, 4836 (1975).
- ³²G. Martens, P. Rabe, N. Schwentner, and A. Werner, *Phys. Rev. Lett.* **39**, 1411 (1977).
- ³³R. J. Cava, A. Santoro, D. W. Johnson, Jr., and W. W. Rhodes, *Phys. Rev. B* **35**, 6716 (1987).
- ³⁴J. D. Jorgensen, H.-B. Schüttler, D. G. Hinks, D. W. Capone II, K. Zhang, M. B. Brodsky, and D. J. Scalapino, *Phys. Rev. Lett.* **58**, 1024 (1987).
- ³⁵J. B. Boyce, F. Bridges, T. Claeson, T. H. Geballe, C. W. Chu, and J. M. Tarascon, *Phys. Rev. B* **35**, 7203 (1987).
- ³⁶S. Kanbe, K. Kishio, K. Kitazawa, K. Fueki, H. Takagi, and S. Tanaka, *Chem. Lett.* 547 (1987).
- ³⁷R. J. Cava, A. Santoro, D. W. Johnson, Jr., and W. W. Rhodes, *Phys. Rev. B* **35**, 6716 (1987).
- ³⁸U. Schröder, *Solid State Commun.* **4**, 347 (1966).
- ³⁹N. N. Bogoliubov, V. V. Tolmachev, and D. V. Shirkov, *A New Method in the Theory of Superconductivity* (Academy of Science, Moscow, 1958), translated by Consultants Bureau, New York, 1959.
- ⁴⁰V. J. Emery (private communication).